Spatio-temporal variation of bacterial community structure in two intertidal sediment types of Jiaozhou Bay

Xuechao Chen [a,#], Xinran Zhang [a,#], Hao Yu [a,#], Meiaoxue Han [a], Jianhua Sun [a], Gang Liu [a], Yan Ji [a], Chuan Zhai [b], Liyan Zhu [c], Hongbing Shao [a,d], Yantao Liang [a,d,*], Andrew McMinn [a,b,*], Min Wang [a,d,e,f,*]

a College of Marine Life Sciences, Institute of Evolution and Marine Biodiversity, Frontiers Science Center for Deep Ocean Multispheres and Earth System, Center for Ocean Carbon Neutrality, Ocean University of China, Qingdao 266003, China

b Institute for Marine and Antarctic Studies, University of Tasmania, Hobart, TAS 7001, Australia

c College of Marine Life Sciences, Ocean University of China, Qingdao 266003, China

d UMT-OUC Joint Centre for Marine Studies, Qingdao 266003, China

e Haide College, Ocean University of China, Qingdao 266003, China

f The Affiliated Hospital of Qingdao University, Qingdao 266000, China

#: These authors contributed equally to this work (X. Chen, X. Zhang and H. Yu).

*: Corresponding author, E-mail addresses: mingwang@ouc.edu.cn (M. Wang), andrew.mcminn@utas.edu.au (A. McMinn), liangyantao@ouc.edu.cn (Y. Liang)

Graphic abstract

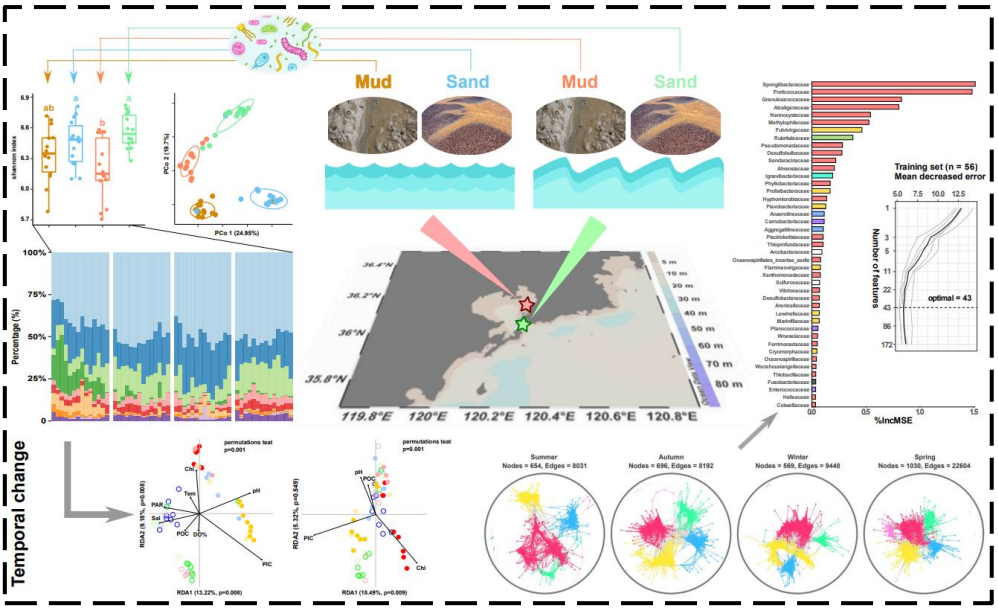

Highlights:

- Sandy sediments have more bacterial species involved in community building.
- Different substrates from different stations have their own phylum biomarkers.
- Substrates have a greater influence on shaping bacterial function.
- Temporal changes have a greater shaping power on bacteria than on gene families.

Abstract: The intertidal sediment environment is dynamic and the biofilm bacterial community within it must constantly adjust, but an understanding of the differences in the biofilm bacterial community within sediments of different types is still relatively limited. In this study, the structure of the bacterial community in Jiaozhou Bay sediment biofilms are described using high-throughput 16S rRNA gene sequencing and the effects of temporal change and different sediment environment types are discussed. The Shannon index was significantly higher in sandy samples than in muddy samples. The co-occurrence network was tighter and more species were involved in community building in sandy samples. The principal coordinates analysis identified a significant separation between different sediment types and between stations (LiCun estuary, LC and ZhanQiao Pier, ZQ).

Proteobacteria, which had a relative abundance of approximately 50% at all phylum levels, was significantly more abundant at ZQ, while Campilobacterota and Firmicutes were significantly more abundant at LC. The relative abundances of Bacteroidetes, Campilobacterota, Firmicutes, and Chloroflexi were significantly higher in the muddy samples, while Actinobacteria and Proteobacteria were higher in the sandy samples. There were different phylum-level biomarkers between sediment types at different stations. There were also different patterns of functional enrichment in biogeochemical cycles between sediment types and stations with the former having more gene families that differed significantly, highlighting their greater role in determining bacterial function. The RDA results, where each month's samples were concentrated individually, showed reduced variation between months when the amplicon sequence variant was replaced by KEGG orthologs, presumably the temporal change had an impact on shaping the intertidal sediment bacterial community, although this was less clear at the gene family level. Random forest prediction yielded a combination of 43 family-level features that responded well to temporal change, reflecting the influence of temporal change on sediment biofilm bacteria.

Keywords: Biofilm; Seasonal variation; Grain size; LEfSe; Gene function

1 Introduction

The intertidal zone is a transition zone between land and sea where the sediment environment is constantly changing under the combined influence of freshwater, tidal and anthropogenic factors. Studies have shown that the sediment surface has high microbial activity, which is sensitive to environmental changes and can be an indicator of ecological health (Duarte et al., 2012; Kallmeyer et al., 2012; Suh et al., 2015; Yi et al., 2020). In addition to microorganisms on the surface of

intertidal sediments that adhere and aggregate into marine biofilms, marine biofilms are also widespread on the surface of other biotic or abiotic substrates immersed in seawater and play an important role in biogeochemical cycles (Wahl et al., 2012; Dang and Lovell, 2016; Liang et al., 2019).

Bacteria are the pioneer and most abundant taxa in biofilms, and their diversity and aggregation state are significantly influenced by water quality, salinity and hydrodynamics (Rickard et al., 2004; Nocker et al., 2007; Qian et al., 2007; Guo et al., 2017). Rapid fluctuations in intertidal environmental conditions (e.g., pH, salinity, ionic strength, currents and contaminants) result in a metabolically plastic and genetically diverse community of bacteria. Understanding how changes in the distribution and function of these communities and the extent to which anthropogenic and natural factors influence them is essential for assessing ecological impacts (Lv et al., 2016; Wei et al., 2018; Avila-Jimenez et al., 2020; Ge et al., 2021). With the development and maturity of sequencing technology, in particular using high-throughput 16S rRNA gene sequencing technology, it has become possible to study community composition at a lower cost, with greater accuracy and efficiency.

Tidal, current and invertebrate disturbance have different effects on the erosion of the surface layer of intertidal sediments with different grain sizes (Grabowski et al., 2011). Sandy sediments have high permeability but low interparticle cohesion, whereas muddy sediments have smaller particle sizes, higher cohesion and increased stability, so surface migration differs between the two sediment types. In addition, sediment mobility is also influenced by the biofilms themselves (Paterson, 1989; Whitehouse, 2000; Wyness et al., 2019). However, an understanding of the structural differences in intertidal biofilm bacterial communities in different substrate types is still

77 relatively limited. Therefore, it is hypothesised that intertidal muddy and sandy sediments shape
78 bacterial communities differently. In this study, Jiaozhou Bay, a temperate bay with different
79 sediment types, was chosen as a study model.

80 Jiaozhou Bay (Shandong, China) is a semi-enclosed bay with a relatively narrow mouth (2.5
81 km) that restricts water exchange to the Yellow Sea and limits its capacity to self-purify (Dai et al.,
82 2007; Sun et al., 2021). It's semi-enclosed configuration results in low wave energy. It has a
83 temperate monsoon climate, semi-diurnal tides (mean tidal range 2.8 m) and high current velocities
84 (up to 201 cm/s) at the mouth of the bay (Lyu et al., 2010; Liu et al., 2014; Shang et al., 2018). The
85 Licun River, which flows into the bay, has a population of more than one million people within its
86 catchment. A large sewage treatment plant discharges into the Licun River (2.46×10^5 t/d). A eddy
87 in the estuary attenuates the movement of material out of the bay (Wang et al., 2022; Zhang et al.,
88 2017). Previous studies have investigated the diversity of culturable bacteria (Wang et al., 2016),
89 the diversity of anaerobic bacteria (Wu et al., 2019), the *nirS*-type denitrifying bacterial community
90 (Liu et al., 2020), the late winter/early spring bacterial community in the estuarine zone (Ge et al.,
91 2021), and the spatial distribution of bacteria in autumn (Sun et al., 2021) in surface sediments of
92 Jiaozhou Bay, but investigations of bacterial community structure between seasons and substrates
93 are need to be complemented.

94 In a monthly sampling program for almost a year, the bacterial community structure of the
95 intertidal sediments in the bay and at the mouth of the bay is described using high-throughput 16S
96 rRNA gene sequencing methods. The aim is to identify potential patterns in the composition of
97 bacterial communities in the sediment biofilms, and the effects of temporal changes and sediment
98 environment on them. The results will improve our understanding of the endemic structure of

bacterial communities shaped by different substrate sediments in the intertidal zone and provide the empirical support necessary for ecological conservation.

2 Materials and Methods

2.1 Sampling design

The sampling sites were at two locations in Jiaozhou Bay - the south side of the LiCun estuary (LC, 36.15 N 120.34 E) and a beach on the east side of the ZhanQiao Pier (ZQ, 36.06 N 120.31 E), inside and outside the mouth of the bay respectively, a linear separation of approximately 10.5 km. Samples were collected monthly over a period of 326 days (Fig. 1). Sampling preferentially took place when low tides (<90 cm) occurred close to midday. Surface samples (0.5 cm) were collected from different sediment types (muddy samples, sandy samples). The samples from each site were collected close to the water's edge (where the samples were only exposed to air for a short time, resulting in less water loss and less additional stress), divided into collection tubes for cold storage at -80 °C in the laboratory. Water temperature (Tem), dissolved oxygen air saturation (DO%), dissolved oxygen (DO), total dissolved solids (TDS), salinity (Sal), pH of the seawater adjacent to the sediment were measured *in situ* using a YSI water quality analyzer. Photosynthetically active radiation (PAR), chlorophyll (Chl), particulate inorganic carbon (calcite concentration, PIC), particulate organic carbon (POC) were extracted from MODIS-Aqua remote sensing data, and if the extracted values were NA, then extracted from 8-day average, monthly average, etc.

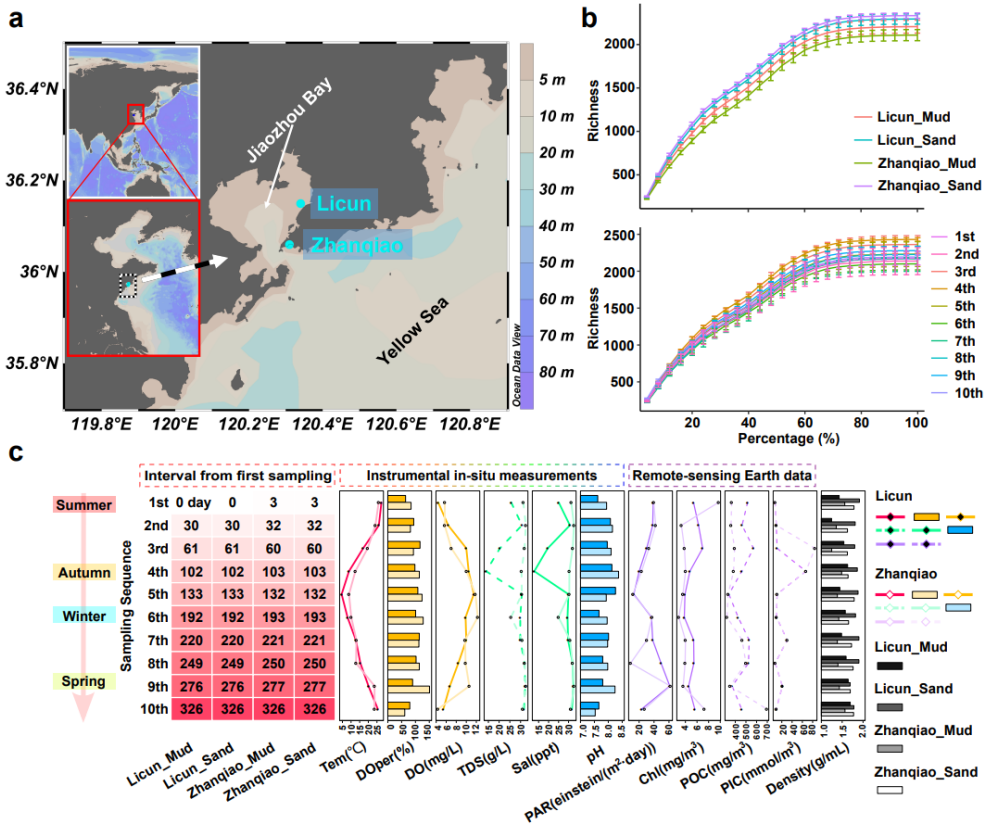

	Licun_Mud	Licun_Sand	Zhanqiao_Mud	Zhanqiao_Sand
1st	0 day	0	3	3
2nd	30	30	32	32
3rd	61	61	60	60
4th	102	102	103	103
5th	133	133	132	132
6th	192	192	193	193
7th	220	220	221	221
8th	249	249	250	250
9th	276	276	277	277
10th	326	326	326	326

Fig. 1 Sampling design. a) Geographical information on the stations b) Richness dilution curve c) Sampling time and variation of environmental factors (Tem: water temperature Doper: dissolved oxygen air saturation DO: dissolved oxygen TDS: total dissolved solids Sal: salinity PAR: photosynthetically active radiation PIC: particulate inorganic carbon POC: particulate organic carbon).

2.2 High throughput sequencing

Samples for sequencing were collected each month, with the August (1st sample month), November (4th), February (6th) and May (9th) being characteristic months of each local season; an additional parallel sample was also sequenced. DNA was extracted from the genomic DNA of the microbial community according to the instructions of the E.Z.N.A.® Soil DNA Kit (Omega Bio-tek, Norcross, GA, USA). 1% agarose gel electrophoresis was used to check DNA quality and

NanoDrop 2000 (Thermo Scientific, USA) was used to determine DNA concentration and purity. PCR amplification of the V3-V4 variable region of the 16S rRNA gene was performed using upstream primer 338F (5'-ACTCCTACGGGAGGCAGCAG-3') and downstream primer 806R (5'-GGACTACHVGGGTWTCTAAT-3') with barcode sequences (Liu et al., 2016), the PCR reaction system was: 5×FastPfu buffer 4 μL, 2.5 mM dNTPs 2 μL, each primer (5 μM) 0.8 μL, Fast Pfu polymerase 0.4 μL, bovine serum albumin (BSA) 0.2 μL, template DNA 10 ng, and ddH2O to a final volume of 20 μL. Amplification procedure: initial denaturation at 95°C for 3 min, 27 cycles (denaturation at 95°C for 30 s, annealing at 55°C for 30 s, extension at 72°C for 45 s), followed by a single extension at 72°C for 10 min (ABI GeneAmp® 9700). Three replicates of each sample were run. PCR products from the same sample were mixed and recovered on a 2% agarose gel, purified using the AxyPrep DNA Gel Extraction Kit (Axygen Biosciences, Union City, CA, USA), quantified using a Quantus™ Fluorometer (Promega, USA) and libraries constructed. Sequencing was performed on the Illumina Miseq PE300 platform (Illumina, San Diego, USA) according to the standard protocol of Majorbio Bio-Pharm Technology Co. Ltd. (Shanghai, China).

2.3 Sequencing data processing

Quality control of the double-ended raw sequencing data was performed using fastp v0.19.6 (Chen et al., 2018). Splicing was performed using FLASH v1.2.11 (Magoč and Salzberg, 2011): 1) truncate window bases for reads with an average quality score <20 within the 50 bp window of the tail, filter reads below 50 bp, and reads containing N bases were removed; 2) splice pairs of reads with a minimum overlap of 10 bp; 3) filter sequences with an overlap mismatch rate >0.2. Barcode and front-end primer sequences were removed. The data have been deposited in the Genome

Sequence Archive (Tingting Chen et al., 2021) in National Genomics Data Center, China National Center (CNCB-NGDC Members and Partners, 2022) for Bioinformation / Beijing Institute of Genomics, Chinese Academy of Sciences (GSA: CRA010554) that are publicly accessible at https://ngdc.cncb.ac.cn/gsa.

Amplicon sequence variant (ASV) selection and feature table construction were performed using EasyAmplicon v1.14 (Liu et al., 2021): in the quality filter, a default value of 0.01 was used for "-fastq_maxee_rate"; in dereplication, a default value of 8 was used for "-miniuniqusize"; in denoising, "- minsize" was set to 20; in the feature table construction, the default statement was used; when removing plastids and non-bacteria, "- db" was set to rdp_16s_v18.fa, "- sintax_cutoff" was set to 0.6; normalization by subsample was set to the minimum value by default.

Alpha diversity was analyzed using EasyAmplicon: box plots and dilution curves were plotted using the default statements; filtering by abundance used a default value of 0 for "-thre", true for "-scale" and 100 for "-zoom"; the default statement was used to filter the results above an abundance threshold (0.1%). The Venn network was plotted using EVenn (Tong Chen et al., 2021).

Beta diversity and relative abundance at the phylum and class level were analyzed using EasyAmplicon: default statements generated bray_curtis distance matrices, PCoA, CPCoA, and stackplot were plotted; in the treemap, "- topN" was set to 200; in the extended histogram, "-threshold" was set to the default value of 0.1, a default value of "t.test" was used for "--method", a default value of 0.05 was used for the "--pvalue", and "BH" was used for "--fdr".

LEfSe analysis was performed using OECloud tools (https://cloud.oebiotech.cn.), with 0.1% abundance screening, unassigned categories were not included in the analysis, for the interclass Kruskal-Wallis test, alpha = 0.05, LDA score threshold was 2.0.

FAPROTAX v1.2.4 (Louca et al., 2016) in ImageGP (Chen et al., 2022) (http://www.ehbio.com/ImageGP/index.php/Home/Index/FAPROTAX.html) was used to predict biogeochemical cycle functional genes and STAMP v2.1.3 (Parks et al., 2014) was used to analyse for significant differences between the two groups: Welch's t-test was used with a Storey FDR test correction. PICRUSt2 (Douglas et al., 2019) in the OECloud tools (https://cloud.oebiotech.cn) was used to predict the abundance of gene families. The volcano plot between the two groups was performed using EasyAmplicon and OmicStudio (Lyu et al., 2023) with "--threshold" set to 0, "--method" set to Wilcox, "--pvalue" set to the default value of 0.05 and "--fdr" set to 0.05. The top 25 enriched/depleted relative abundances in the volcano plot were plotted on a heatmap (R package ComplexHeatmap v2.15.1) (Gu et al., 2016; Gu, 2022).

The R package igraph v1.3.2 (Csardi and Nepusz, 2006) was used to analyze the network modules, calculate the Pearson correlation coefficient between two ASVs (occurrence >80%), maintain a threshold of $r > 0.7$ and $p < 0.01$ and calculate the layout based on layout_with_fr. The 18 modules with the highest number of nodes were colored.

Environmental factor analysis: ASVs (or KEGG orthologs) with station-wide frequencies ≥100 were screened for Hellinger transformation to attenuate the effect of zero values. Environmental factor data were +1 and then natural log transformed to make the data more homogeneous. Using the R package vegan v2.6-2 (Oksanen, 2010) decorana() operations for axis lengths and vif.cca() for covariance analysis, 999 permutation tests were carried out on the constraint axis as a whole and on each axis separately (Bonferroni for p-value correction). ordistep()/ordiR2step() was used for forward selection and 999 permutation tests, varpart() was used for variance decomposition followed by 999 permutation tests to explain variance. bioenv() was used to calculate the most

relevant combination of environmental factors.

Random forest modelling was performed using the R package randomForest v4.7-1.1 with a default statement and with cross-validation to filter the number of features associated with temporal change (Liaw and Wiener, 2002; J. Zhang et al., 2018; Liu et al., 2021). The monthly affiliation of sediment samples was predicted based on the feature model, and a time-series prediction fit was plotted.

3 Results

3.1 Sequence screening and ASV characterization table

After quality control of 56 amplicon samples, 2,606,341 sequences were retained and 296,193 sequences were discarded. 6,723 good amplicons were obtained after redundancy and denoising. 6,497 ASVs were obtained after removal of plasmids and non-bacteria (1,754,033/2,606,341 = 67.3% sequences mapped). Sample size was 15,325 after equal sampling and normalization.

3.2 Alpha diversity

Dilution curves by time series and by station and substrate type each reached a plateau (Fig. 1b). There were no significant differences in the Shannon indices between the monthly samples. The Shannon index for ZQ mud samples was significantly lower than that for ZQ sand samples (TukeyHSD, $p = 0.001$) and significantly lower than that for LC sand samples ($p = 0.036$) (Fig. 2b). There were 432 ASVs with a relative abundance >0.1% by station and substrate type, with 152-181 ASVs in each group. There were 284 ASVs that were unique to each group. There were 1,652 ASVs with abundances >0.1% when counted by temporal variation, with the least variation between

219 samples collected from 5-7th (December, February and March) and the most variation within

220 samples collected from 8-10th (April, May and July).

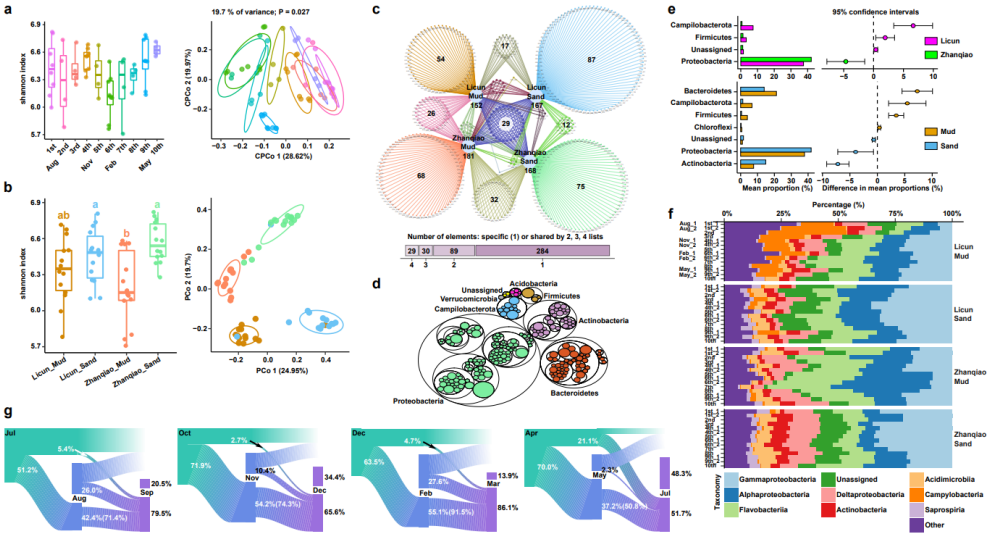

221

222 Fig. 2 Alpha/Beta diversity and relative abundance at major phylum and class levels. a)

223 Shannon index (TukeyHSD test) and CPCoA of samples by month b) Shannon index (TukeyHSD

224 test) and PCoA (Bray_Curtis) of samples from different stations and substrates c) Venn network

225 plots of bacterial ASVs (abundance >0.1%) between stations and substrate types d) Treemap of

226 relative abundance top200 ASVs e) Comparison of differences in phylum levels (abundance >0.1%)

227 between stations and between substrates (>0.5%, t.test, p <0.05) f) Relative abundance at major

228 class levels g) Sankey plots of changes in bacterial ASVs (>0.1%) by season, with transmission

229 rates of common ASVs in brackets.

230

231 3.3 Beta diversity and relative abundance at major phylum and class levels

232 CPCoA analysis of samples from each month was significant at 19.7% resolution (p <0.05)

233 and was best separated on CPCo axis 1. PCoA analyses separated samples from different stations

234 and substrates (p <0.05). Most of the top200 ASVs by relative abundance belonged to

235 Proteobacteria, Bacteroidetes and Actinobacteria. The relative abundance of Campilobacterota and

Firmicutes was significantly higher at LC, while Proteobacteria was significantly higher at ZQ. Bacteroidetes, Campilobacterota, Firmicutes and Chloroflexi were significantly more abundant in the muddy samples, while Actinobacteria and Proteobacteria were significantly more abundant in the sandy samples. The composition at the class level varied between stations and substrates, although Gammaproteobacteria, Alphaproteobacteria, Flavobacteriia were most abundant with the sum of their relative abundances accounting for about 50% (Fig. 2).

3.4 Linear Discriminant Analysis Effect Size (LEfSe) analysis

In the LEfSe of the monthly samples, Verrucomicrobia was the biomarker for the February sample, Bacilli and Verrucomicrobiae for February, Alphaproteobacteria for March, Bacteroidia for August and Cytophagia for October. Among the different stations and substrates, Acidobacteria and Bacteroidetes were biomarkers for the ZQ mud samples, Actinobacteria for ZQ sand, Campilobacterota and Firmicutes for LC mud, and Proteobacteria for LC sand (Fig. 3).

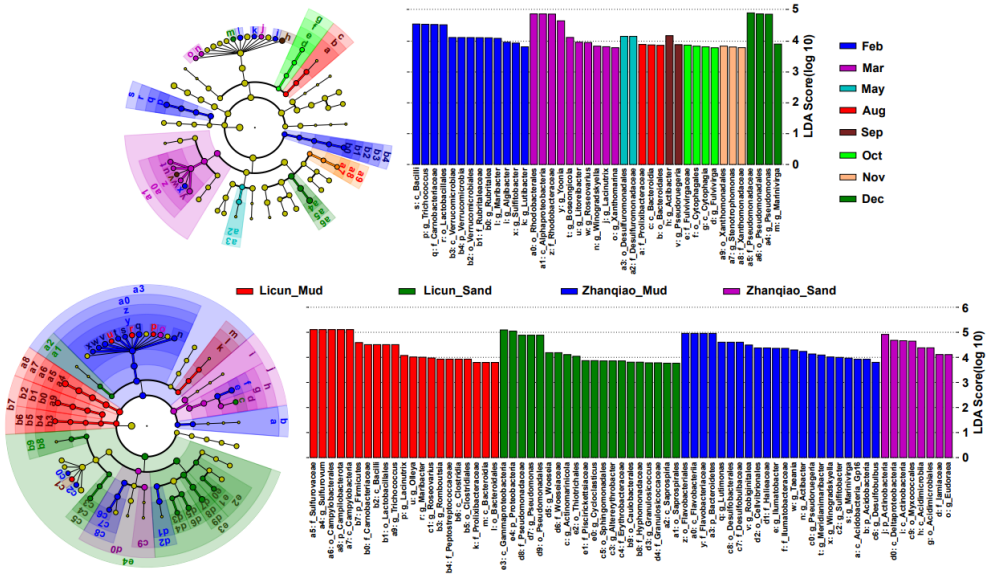

Fig. 3 Time series and station/substrate LEfSe analysis. Dot diameters represent relative abundance (>0.1%, unassigned categories are not included in the analysis), no significant

252 differences are yellow, Kruskal-Wallis tests for significant differences between classes ($p < 0.05$) are
253 assigned colors, LDA score threshold 2.0.
254
255 3.5 Comparison of gene function
256 Chemoheterotrophy function was high at both stations (>30% in all), with significantly higher
257 abundance at LC (34.6%, Welch's t-test, $p = 0.024$). Respiration of sulfur compounds (11.4%) and
258 sulfate respiration (11.2%) were also significantly higher at ZQ ($p < 0.001$). The relative abundance
259 of aerobic chemoheterotrophy was different between substrates, with sandy samples being highly
260 significantly higher (29.7%, $p = 0.0002$). Fermentation abundance was significantly higher in mud
261 samples (9.9%, $p < 0.001$) (Fig. 4).

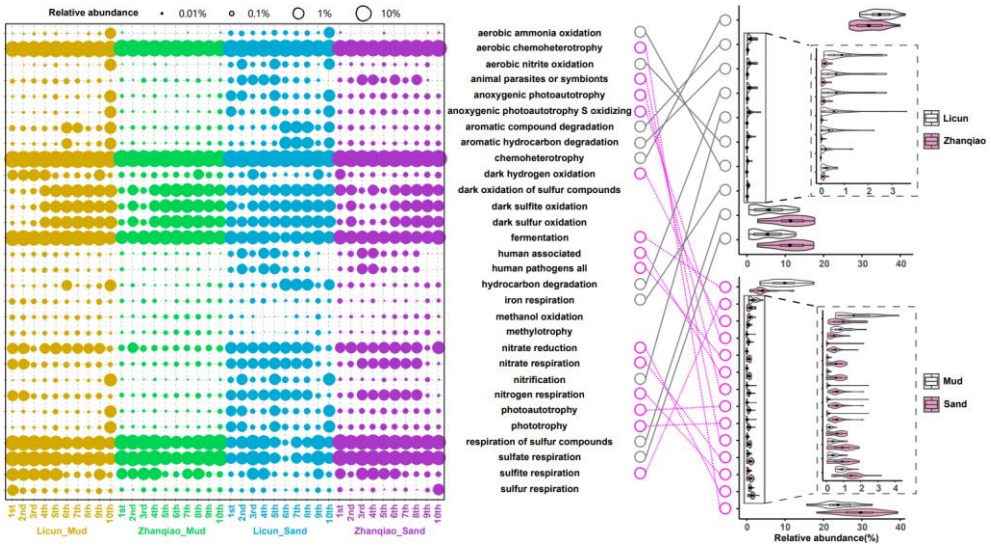

262
263 Fig. 4 Relative abundance of elemental cycling functions (abundance >0.1%) and comparison
264 of differences between stations and between substrates (abundance > 0.2%, Welch's t-test, $p <$
265 0.05).
266
267 Among gene families, the relative abundance of those associated with lipid metabolism,
268 terpenoid metabolism and polyketides was >0.5% and significantly higher at ZQ than at LC.

Between substrates, there were more significantly different KEGG_L2 (Kyoto Encyclopedia of Genes and Genomes, 16 categories with abundance >0.5%) involving metabolism, environmental information processing, cellular processes, organismal systems and human diseases. Most KEGG_L3 (90.2%) were not significantly different between stations, whereas 56.1% were significantly different between substrates (Fig. S3). KEGG orthologs (KO) was also mostly (81.7%) not significantly different between stations, although 64.5% were significantly different between substrates (Fig. 5).

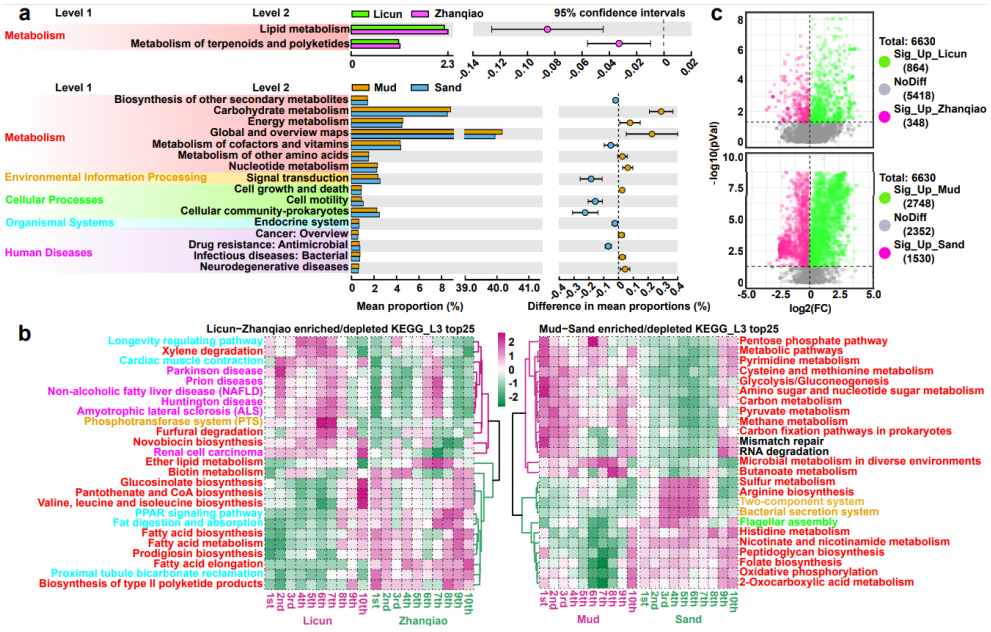

Fig. 5 Gene family prediction. a) Comparison of KEGG differences between stations and substrates (abundance >0.5%, Welch's t.test, adj <0.05) b) Relative abundance of major enriched/depleted KEGG_L3 between stations and substrates (top25, category names colored as in Fig. 5a KEGG_L1) c) KO volcanogram analysis across stations and substrates.

3.6 Comparison of network modularity

The average edge number of nodes with significant correlations in summer, autumn, winter and spring were 12.3, 11.8, 16.6 and 21.9. Within stations, sandy samples have a higher number of

285 nodes and a higher average connectivity degree than muddy samples (LC - muddy 8.6, sandy 11.4,

286 ZQ - muddy 7.2, sandy 14.2) (Fig. 6).

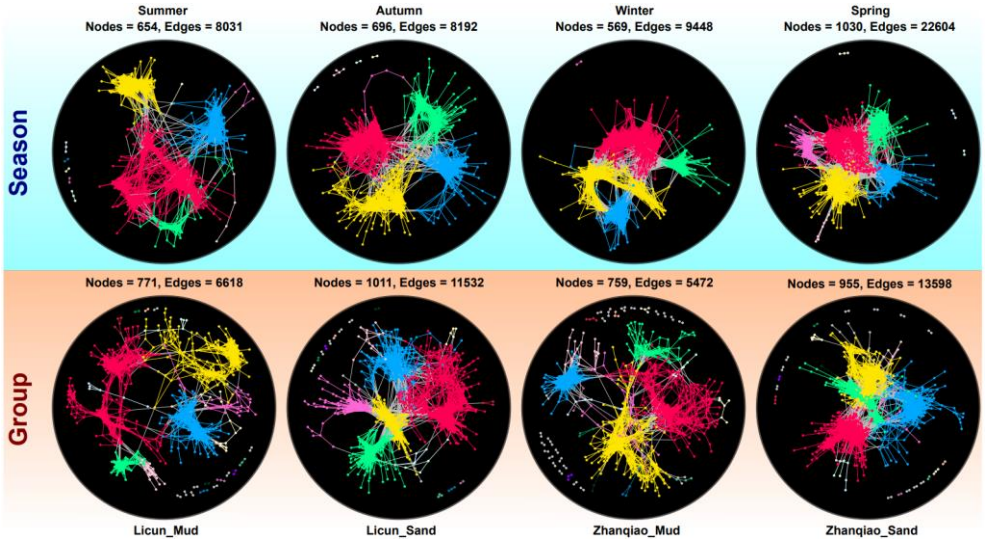

287

288 Fig. 6 Network module analysis. The top row shows the network modules of different seasons;

289 the bottom row shows the network modules of different stations and substrates. The Pearson

290 correlation coefficient ($r > 0.7$ and $p < 0.01$) was calculated between two ASVs with an occurrence

291 rate >80%. The layout was calculated based on layout_with_fr. In each network diagram, the top 18

292 modules are given a different color.

293

294 3.7 Analysis of environmental factors

295 PIC + pH + DO% + PAR + Sal + Tem + POC + Chl were forward selected in this order. The

296 total variance explained by PIC/pH/PAR was significant ($p < 0.05$). The most relevant combination

297 of environmental factors was PIC for size 1 (correlation 0.3154). On the RDA1 axis, there was a

298 tendency for samples to be separated by season (Fig. 7).

299 PIC + pH + Chl + POC passed forward selection in order and the total variance explained by

300 PIC/Chl was significant ($p < 0.01$). The most relevant environmental factor combination was Chl +

301 PIC for size 2 (correlation 0.3103), followed by Chl + PIC + POC for size 3 (0.2870) and Chl for

size 1 (0.2694). There was less variation between samples compared to the results of the ASV redundancy analysis (Fig. 7).

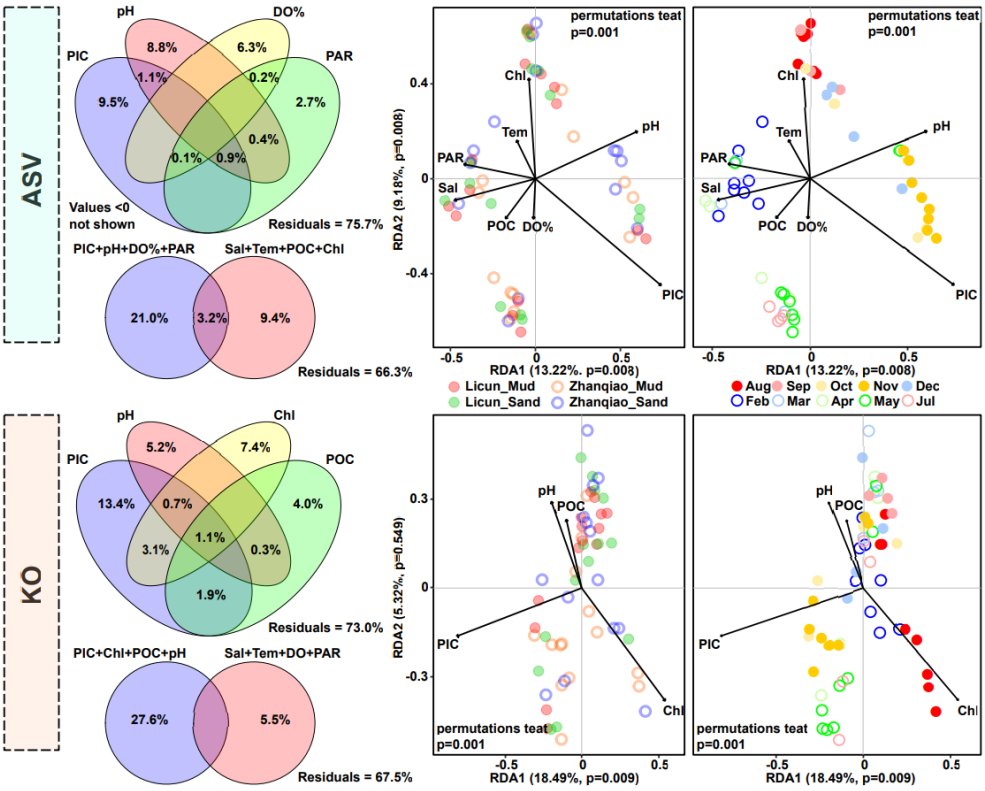

Fig. 7 Environmental factor analysis. Individual and combined variance decomposition of the best four factors in forward selection, parsimonious model after forward selection showing the first two axes of the RDA (type II scale, double ordinate plot, sample coordinates calculated using species weights). Tem: water temperature DO%: dissolved oxygen air saturation Sal: salinity PAR: photosynthetically active radiation PIC: particulate inorganic carbon POC: particulate organic carbon.

3.8 Random forest prediction

Cross-validation yielded 43 family-level features that were the better combinations, with the Proteobacteria of spongiibacteraceae, porticoccaceae, granulosicoccaceae, alcaligenaceae,

316 nannocystaceae and methylophilaceae having the highest importance (%IncMSE) (Fig. S5).

317

318 **4 Discussion**

319 4.1 Relationship between intertidal sediment biofilms by station and substrate factors

320 The Shannon index did not differ significantly between stations, but was less variable and
321 significantly higher in sandy samples than in muddy samples (Fig. S1). A comparison of network
322 modularity also showed that the correlations between the ASVs were tighter and that there were
323 more ASVs involved in community assembly in sandy samples than in mud (Fig. 6). Network
324 complexity and connectivity are often positively correlated with environmental heterogeneity and
325 microbial communities in heterogeneous environments are more likely to aggregate and form
326 cooperative networks to share resources and transfer information (Mougi and Kondoh, 2012;
327 Morriën et al., 2017; Lu et al., 2022). It is hypothesized here that differences in current strength and
328 runoff within and outside the bay may have had a stronger effect on permeable sandy sediments,
329 with increased heterogeneity promoting bacterial aggregation to adapt to the environment.

330 Of the highly abundant bacteria in each station/substrate type, ASVs unique to each group
331 accounted for 35.5-52.1% of the groups, indicating variability in the composition of high abundance
332 bacteria in each sample group, even between samples of different substrates sampled in close
333 proximity within stations. Bacterial diversity has been found to differ between fine- and coarse-
334 grained sediments (Lai et al., 2023). Differences in sediment grain structure can also lead to changes
335 in bacterial community structure (van de Kamp et al., 2019). The abundance of nitrification-
336 associated bacteria fluctuates more in intertidal sandy sediments than in mud (Fernandes et al.,
337 2016). Sediment grain size has a significant effect on the community structure of *nirS*-type

338 denitrifying bacteria (Chen et al., 2020). Therefore, sediments of different grain sizes have the
339 ability to shape their own specific bacterial communities.

340 Proteobacteria were the most abundant group in this study, accounting for about 50% (Fig. S2).
341 They were slightly less abundant in LC mud samples (especially in summer, when Campilobacterota
342 appeared in high abundance, increasing from an average of 1.2% to 14.6-34.1%). Proteobacteria are
343 widely distributed, have high metabolic, cooperative and biofilm-forming capacities, and are also
344 adapted to high metal loads (Regnell and Watras, 2019; Zhuang et al., 2019; Hillyer et al., 2023).
345 Proteobacteria have been detected in high abundance in estuarine intertidal sediments (37.5%) (Yi
346 et al., 2020), coral reef sediments (65%) (Alvarez-Yela et al., 2019), mangrove surface sediments
347 (>40%) (Huergo et al., 2018; Fiard et al., 2022), polar surface sediments (44-68%) (Thomas et al.,
348 2020; Chaudhary et al., 2022), and marine sediments exposed to oil transport activities (45-77%)
349 (Oyetibo et al., 2021). Campilobacterota has been observed at higher abundances (>5%) in
350 thermogenic hydrocarbon seep sediments (Li et al., 2023) and is involved in mediating oxidation of
351 sulfur, sulfide or sulphate in intertidal sediments (7.90-22.15%) (Carrier et al., 2020; Fang et al.,
352 2022). The genus Arcobacter has been found to increase in abundance in anoxic surface sediments,
353 and in addition, is highly responsive to oxygenation events (Broman et al., 2017; Mori et al., 2021).
354 Therefore, it is likely that hydrocarbon, sulfide and oxygen (low summer oxygen, low mud
355 permeability and low circulation rates within the bay) are responsible for the increased abundance
356 of Campilobacterota in summer mud samples at LC.

357 There are corresponding phylum-level biomarkers in different stations and substrates. All
358 taxonomic levels of Firmicutes and Campilobacterotas were biomarkers in LC mud samples,
359 Firmicutes is one of the major groups in natural biofilms (Guo et al., 2017; Liang et al., 2019) and

is abundant in polyethylene microplastic biofilms, and may provide potential hosts for antibiotic resistance genes (Wu et al., 2017; Guo et al., 2020). Firmicutes is also highly abundant in environments under severe stress, such as in deep-sea sediments (9.5%) (Goffredi and Orphan, 2010; Franco et al., 2020), shallow hypoxic zone sediments (Bhattacharya et al., 2021), and anaerobic bioreactors (involved in hydrolysis and fermentation) (Narihiro et al., 2015; Fontana et al., 2016; Luo et al., 2016). The abundance of all taxonomic levels of Acidobacteria increased in ZQ mud samples and most were also increased in ZQ sand samples. Acidobacteria are low-nutrient bacteria (Fierer et al., 2007) that have been found to be adapted to polar environments (Pearce et al., 2013; Gugliandolo et al., 2016) and are key microorganisms (~8%) in mangrove sediments (Huergo et al., 2018; Tavares et al., 2021; Fiard et al., 2022). Actinobacteria is one of the major bacterial groups in estuarine surface sediments and is significantly and positively correlated with denitrification rates (Wei et al., 2015; Li et al., 2022). Uncultured Actinobacteria OPB41 has been shown to be adapted to deep-sea sediment environments, where it can catabolize sugars and be metabolically active (Zinke et al., 2017; Bird et al., 2019). In summary, there were significant differences in the abundance patterns of the more diverse bacterial taxa and functions between the different stations and substrates, shaping their own specific bacterial communities.

Chemoheterotrophy function occurred in 77.8% (900 of 1,157 ASVs) and aerobic chemoheterotrophy function occurred in 58.5%. One study has found that the abundance of chemoheterotrophy and aerobic chemoheterotrophy in surface sediments may account for up to half of the total abundance, giving bacteria a strong ability to degrade organic matter and obtain energy from the oxidation of organic compounds (X. Zhang et al., 2018; Hou et al., 2021). Chemoheterotrophy and aerobic chemoheterotrophy account for more than 50% of the bacteria

382 and probably point to a stronger tendency for organic matter degradation in LC or sandy
383 sediments. Sulfur compounds respiration function occurred in 26.4% (306 of 1,157 ASVs) and
384 sulfate respiration function occurred in 24.4% (282 of 1,157 ASVs). Sulfur compounds respiration
385 may be associated with adaptation to hypoxia by promoting respiration using sulfides as electron
386 acceptors (Deng et al., 2019). Sulfate respiration may play a major role in the biodegradation of
387 sulfate-dependent aromatic compounds (Zhuang et al., 2019). Fermentation function occurred in
388 22.0% (255 of 1,157 ASVs). It has been found that microorganisms in intertidal and subtidal
389 sandy sediments often switch between oxic and anoxic states, favouring facultative anaerobic
390 fermenters where fermentation is dominated by anoxic carbon mineralization (which also
391 promotes H_2 production), in contrast to muddy sediments where it is largely unrelated to anaerobic
392 respiration (Precht et al., 2004; Kessler et al., 2013; Saad et al., 2017; Kessler et al., 2019).
393 Fermentation also promotes the cycling of other material, such as in organic matter-rich and
394 sulfate-rich environments, where enhanced fermentation may lead to increased microbial
395 reduction of sulfate (Sun et al., 2020). The abundant biogeochemical cycling functions differ
396 significantly between stations and substrates, with stations mostly differing significantly in
397 chemoheterotrophy, sulphur, nitrogen, iron, aromatics and hydrocarbon metabolism, whereas
398 substrates differ in aerobic chemoheterotrophy, fermentation, dark hydrogen oxidation, animal-
399 related, photosynthesis-related and sulphite metabolism, suggesting that both station and substrate
400 factors are likely to be differentially involved in biogeochemical cycling processes between
401 samples.

402 There were significantly fewer categories of significant differences between stations than
403 between substrates in KEGG_L2, suggesting that differences in gene functions were more due to

404 substrate differences than to differences in location within and outside the bay. Between stations,
405 the enriched/depleted KEGG_L3 top25 involved more organismal systems and human diseases (Fig.
406 5b), with all human disease categories enriched at LC, suggesting that the poor circulation in the
407 bay was not conducive to effective dispersal of land-based sources of domestic sewage, etc. Between
408 the substrates, the top 25 gene functions were mostly related to metabolism. Significant differences
409 in KO PCoA were found between LC substrates and between muddy samples (Fig. S4). ZQ current
410 velocities subjected the sediments to strong scouring, which promoted similar bacterial gene family
411 succession for both muddy and sandy samples. The low current velocities in the bay may have been
412 sufficient to influence bacterial succession in the more permeable sandy sediments, so that there
413 were no gene family differences between stations for the sandy samples. In contrast, the sediment
414 environment had less influence on gene families than on ASVs, possibly indicating that the bacterial
415 community was evolving but the core gene functions adapted to the environment were relatively
416 stable.
417
418 4.2 Temporal changes in intertidal sediment biofilms
419 Temporal changes in bacterial community structure varies between intertidal and supratidal
420 environments in different areas, with some showing no significant changes and others showing
421 significant shifts (Taylor and Kurtz, 2020). Seasonal changes in bacterial communities are
422 sometimes not as large as spatial changes, when seasonal changes are only apparent in individual
423 taxa (Dini-Andreote et al., 2014; Tebbe et al., 2022). In contrast, bacterioplankton in the Chesapeake
424 Bay have a repeating annual pattern, with strong temporal variation in bacterial communities even
425 overwhelming spatial patterns (Wang et al., 2020). In other estuarine and coastal waters, temporal

426 variation also strongly influences changes in bacterial abundance (Lindh et al., 2015; Bunse and
427 Pinhassi, 2017; Thomson et al., 2022). Bacterioplankton in estuarine wetlands have a high diversity
428 index in summer, and DO and pH strongly influence these communities (Li et al., 2020). In another
429 study of mangrove and tidal wetland sediments, bacterial diversity indices were also higher in
430 summer (Zhou et al., 2017). Dry-rainy season variation was the dominant factor influencing these
431 communities, with temporal and spatial patterns more pronounced in water column bacterial
432 communities than in sediments (Kaestli et al., 2017). In another study, intertidal sediment bacteria
433 were significantly separated in PCoA when grouped by wet and dry seasons (Yi et al., 2020). There
434 is also indirect evidence for the influence of temporal variation on bacterial communities: acyl-
435 homoserine lactones (AHLs), which are key bacterial signals within biofilms that are degraded by
436 pH- and temperature-dependent hydrolysis, vary seasonally in concentration, being higher in winter
437 and lower in summer (Roggatz and Parsons, 2022). The intertidal filter-feeding clam (*Ruditapes*
438 *philippinarum*) is closely related to the microorganisms in its environment, and its extrapallial fluids
439 show strong temporal variation in bacterial alpha-diversity between months (Offret et al., 2023).

440 Of the most abundant bacteria, the least variation over time was seen in winter and the greatest
441 variation in spring (Fig. 2g). Samples collected from April to July were also the most distinct from
442 each other in the CPCoA. In the network modularity comparison, winter and spring samples were
443 more closely correlated than summer and autumn ASVs, with the lowest number of nodes in winter
444 (569) and the highest in spring (1,030) (Fig. 6). Based on the projection of samples on environmental
445 factors by month in the RDA, it is clear that spring samples (April to July samples) were most
446 positively influenced by POC, DO%, PIC and Sal (and most negatively influenced by Tem/Chl/PH),
447 summer samples (August and September samples) were positively influenced by Chl/Tem (and

448 negatively influenced by PIC/DO%/POC), autumn samples (October to December samples) were
449 positively influenced by pH/PIC (and negatively influenced by Sal/PAR) and winter samples
450 (February and March samples) were positively influenced by PAR/Sal (and negatively influenced
451 by pH) (Fig. 7). The spring season was affected by a combination of more environmental factors
452 and the abundant bacteria correlated with each environmental factor varied. The network diagram
453 suggests that the most species were involved in community building in spring, so there was a
454 tendency for greater species variation with environmental changes, whereas in winter the bacteria
455 were more closely related, but had the least number of community building species, so the tendency
456 for variation might be minimal.

457 Monthly samples generally had their own biomarkers at the order level: August - Bacteroidales,
458 October - Cytophagales, November - Xanthomonadales, December - Pseudomonadales, February -
459 Verrucomicrobiales and Lactobacillales, March - Rhodobacterales, and May - Desulfuromonadales.
460 It can be seen that the temporal change had a strong influence in shaping the intertidal bacterial
461 community in the temperate Jiaozhou Bay, and there was a tendency for taxonomic abundance at
462 the order level to change from month to month. The pattern of change in abundance of the better
463 combination in the random forest prediction responded better to changes in temporal change (rho >
464 0.7, $p < 0.001$, $R^2 > 0.6$), reflecting the effect of temporal change on bacterial communities from the
465 other side.

466 The trend of seasonal separation of ASV in the RDA analysis was reduced in the KO analysis.
467 Similar results were also found for CPCoA (Fig. S4). It has previously been reported that when there
468 were seasonal changes in the bacterial community structure in the Monterey Bay upwelling zone,
469 there was a consistent seasonal trend in the gene abundance of key metabolic pathways (Reji et al.,

2020). Bacterial communities in surface waters of Kuwait Bay and nearby coastal waters showed significant seasonal separation, while PICRUSt functional predictions showed partial seasonality (Ismail and Almutairi, 2022). Thus, temporal change had a major influence in the Qingdao intertidal bacterial community, but seems to have had less influence in shaping the gene family of the community.

5 Conclusion

The analyses presented here show that sandy intertidal sediments have more bacterial species involved in community building than muddy sediments. Greater current strengths over the permeable sandy sediments and high environmental stress increased heterogeneity, which in turn promoted bacterial community aggregation and their ability to adapt to the environment. There was a significant separation between substrate types in the PCo 1 axis and between stations in the PCo 2 axis. Different substrate types at the different stations had their own phylum-level biomarkers and bacterial functional enrichment status, with substrate factors having a greater influence. Notably, many gene families associated with human disease were enriched at LC, suggesting that the low circulation rates in the bay were unable to remove contamination from the sources of domestic wastewater. The sediment environment had less influence on KO than on ASV, and it is possible that bacterial species are constantly evolving, but the function of genes adapted to the environment is relatively stable. Temporal changes had a stronger shaping effect on the composition of bacterial species than on gene families. These results will provide the necessary empirical support for ecological conservation in temperate intertidal sediments.

Author contributions

Xuechao Chen, Xinran Zhang, Hao Yu: Methodology, Software, Validation, Formal analysis, Investigation, Project administration, Visualization, Writing - original draft. **Meiaoxue Han, Jianhua Sun , Gang Liu**: Software, Investigation, Writing - review and editing. **Yan Ji , Chuan Zhai , Liyan Zhu**: Writing - review and editing. **Hongbing Shao**: Resources, Supervision. **Min Wang, Andrew McMinn, Yantao Liang**: Conceptualization, Resources, Funding acquisition, Supervision, Writing - review and editing.

Declaration of interests

The authors declare that they have no known competing financial interests or personal relationships that could have appeared to influence the work reported in this paper.

Acknowledgements

We are grateful for the use of the high-performance server at the Center for High Performance Computing and System Simulation, Pilot National Laboratory for Marine Science and Technology (Qingdao, China). We appreciate the computational resources provided by IEMB-1, a high-performance computing cluster operated by the Institute of Evolution and Marine Biodiversity, and the Marine Big Data Center of the Institute for Advanced Ocean Study of Ocean University of China. The data were also analyzed on the free online platform of Majorbio I-Sanger Cloud Platform (www.i-sanger.com) and OECloud tools (https://cloud.oebiotech.cn).

This work was supported by the Laoshan Laboratory (No. LSKJ202203201), National Key

514 Research and Development Program of China (2022YFC2807500), Natural Science Foundation of
515 China (No. 42120104006, 41976117 and 42176111) and the Fundamental Research Funds for the
516 Central Universities (202172002, 201812002, 202072001 and Andrew McMinn).

517

518 References

519 Alvarez-Yela, A.C., Mosquera-Rendón, J., Noreña-P, A., Cristancho, M., López-Alvarez, D., 2019. Microbial
520 diversity exploration of marine hosts at Serrana Bank, a coral atoll of the Seaflower Biosphere Reserve. Front. Mar.
521 Sci. 6, 338. https://doi.org/10.3389/fmars.2019.00338
522 Avila-Jimenez, M.-L., Burns, G., He, Z., Zhou, J., Hodson, A., Avila-Jimenez, J.-L., Pearce, D., 2020. Functional
523 associations and resilience in microbial communities. Microorganisms 8, 951.
524 https://doi.org/10.3390/microorganisms8060951
525 Bhattacharya, S., Mapder, T., Fernandes, S., Roy, C., Sarkar, J., Rameez, M.J., Mandal, S., Sar, A., Chakraborty,
526 A.K., Mondal, N., Chatterjee, S., Dam, B., Peketi, A., Chakraborty, R., Mazumdar, A., Ghosh, W., 2021.
527 Sedimentation rate and organic matter dynamics shape microbiomes across a continental margin. Biogeosciences 18,
528 5203–5222. https://doi.org/10.5194/bg-18-5203-2021
529 Bird, J.T., Tague, E.D., Zinke, L., Schmidt, J.M., Steen, A.D., Reese, B., Marshall, I.P.G., Webster, G., Weightman,
530 A., Castro, H.F., Campagna, S.R., Lloyd, K.G., 2019. Uncultured microbial phyla suggest mechanisms for multi-
531 thousand-year subsistence in Baltic Sea sediments. mBio 10, e02376-18. https://doi.org/10.1128/mBio.02376-18
532 Broman, E., Sachpazidou, V., Pinhassi, J., Dopson, M., 2017. Oxygenation of hypoxic coastal Baltic Sea sediments
533 impacts on chemistry, microbial community composition, and metabolism. Front. Microbiol. 8, 2453.
534 https://doi.org/10.3389/fmicb.2017.02453
535 Bunse, C., Pinhassi, J., 2017. Marine bacterioplankton seasonal succession dynamics. Trends Microbiol. 25, 494–
536 505. https://doi.org/10.1016/j.tim.2016.12.013
537 Carrier, V., Svenning, M.M., Gründger, F., Niemann, H., Dessandier, P.-A., Panieri, G., Kalenitchenko, D., 2020.
538 The impact of methane on microbial communities at marine arctic gas hydrate bearing sediment. Front. Microbiol.
539 11, 1932. https://doi.org/10.3389/fmicb.2020.01932
540 Chaudhary, D.K., Karki, H.P., Bajagain, R., Kim, H., Rhee, T.S., Hong, J.K., Han, S., Choi, Y.-G., Hong, Y., 2022.
541 Mercury and other trace elements distribution and profiling of microbial community in the surface sediments of East
542 Siberian Sea. Mar. Pollut. Bull. 185, 114319. https://doi.org/10.1016/j.marpolbul.2022.114319
543 Chen, Q., Fan, J., Ming, H., Su, J., Wang, Y., Wang, B., 2020. Effects of environmental factors on denitrifying
544 bacteria and functional genes in sediments of Bohai Sea, China. Mar. Pollut. Bull. 160, 111621.
545 https://doi.org/10.1016/j.marpolbul.2020.111621
546 Chen, S., Zhou, Y., Chen, Y., Gu, J., 2018. fastp: an ultra-fast all-in-one FASTQ preprocessor. Bioinformatics 34,
547 i884–i890. https://doi.org/10.1093/bioinformatics/bty560
548 Chen, Tingting, Chen, X., Zhang, S., Zhu, J., Tang, B., Wang, A., Dong, L., Zhang, Zhewen, Yu, C., Sun, Yanling,
549 Chi, L., Chen, H., Zhai, S., Sun, Yubin, Lan, L., Zhang, X., Xiao, J., Bao, Y., Wang, Y., Zhang, Zhang, Zhao, W.,
550 2021. The Genome Sequence Archive Family: Toward Explosive Data Growth and Diverse Data Types. Genomics
551 Proteomics Bioinformatics 19, 578–583. https://doi.org/10.1016/j.gpb.2021.08.001
552 Chen, T., Liu, Y., Huang, L., 2022. ImageGP: An easy-to-use data visualization web server for scientific researchers.

553 iMeta 1. https://doi.org/10.1002/imt2.5
554 Chen, Tong, Zhang, H., Liu, Y., Liu, Y.-X., Huang, L., 2021. EVenn: Easy to create repeatable and editable Venn
555 diagrams and Venn networks online. J. Genet. Genomics 48, 863–866. https://doi.org/10.1016/j.jgg.2021.07.007
556 CNCB-NGDC Members and Partners, 2022. Database resources of the national genomics data center, china national
557 center for bioinformation in 2022. Nucleic Acids Res. 50, D27–D38. https://doi.org/10.1093/nar/gkab951
558 Csardi, G., Nepusz, T., 2006. The igraph software package for complex network research. InterJournal Complex
559 Syst. 1695, 1–9.
560 Dai, J., Song, J., Li, X., Yuan, H., Li, N., Zheng, G., 2007. Environmental changes reflected by sedimentary
561 geochemistry in recent hundred years of Jiaozhou Bay, North China. Environ. Pollut. 145, 656–667.
562 https://doi.org/10.1016/j.envpol.2006.10.005
563 Dang, H., Lovell, C.R., 2016. Microbial surface colonization and biofilm development in marine environments.
564 Microbiol. Mol. Biol. Rev. 80, 91–138. https://doi.org/10.1128/MMBR.00037-15
565 Deng, J., Auchtung, J.M., Konstantinidis, K.T., Brettar, I., Höfle, M.G., Tiedje, J.M., 2019. Genomic variations
566 underlying speciation and niche specialization of *Shewanella baltica*. mSystems 4, e00560-19.
567 https://doi.org/10.1128/mSystems.00560-19
568 Dini-Andreote, F., de Cássia Pereira e Silva, M., Triadó-Margarit, X., Casamayor, E.O., van Elsas, J.D., Salles, J.F.,
569 2014. Dynamics of bacterial community succession in a salt marsh chronosequence: evidences for temporal niche
570 partitioning. ISME J. 8, 1989–2001. https://doi.org/10.1038/ismej.2014.54
571 Douglas, G.M., Maffei, V.J., Zaneveld, J., Yurgel, S.N., Brown, J.R., Taylor, C.M., Huttenhower, C., Langille, M.G.I.,
572 2019. PICRUSt2: An improved and customizable approach for metagenome inference (preprint). Bioinformatics.
573 https://doi.org/10.1101/672295
574 Duarte, B., Freitas, J., Caçador, I., 2012. Sediment microbial activities and physic-chemistry as progress indicators
575 of salt marsh restoration processes. Ecol. Indic. 19, 231–239. https://doi.org/10.1016/j.ecolind.2011.07.014
576 Fang, J., Jiang, W., Meng, S., He, W., Wang, G., Guo, E., Yan, Y., 2022. Polychaete bioturbation alters the taxonomic
577 structure, co-occurrence network, and functional groups of bacterial communities in the intertidal flat. Microb. Ecol.
578 https://doi.org/10.1007/s00248-022-02036-2
579 Fernandes, S.O., Javanaud, C., Michotey, V.D., Guasco, S., Anschutz, P., Bonin, P., 2016. Coupling of bacterial
580 nitrification with denitrification and anammox supports N removal in intertidal sediments (Arcachon Bay, France).
581 Estuar. Coast. Shelf Sci. 179, 39–50. https://doi.org/10.1016/j.ecss.2015.10.009
582 Fiard, M., Cuny, P., Sylvi, L., Hubas, C., Jézéquel, R., Lamy, D., Walcker, R., El Houssainy, A., Heimbürger-Boavida,
583 L.-E., Robinet, T., Bihannic, I., Gilbert, F., Michaud, E., Dirberg, G., Militon, C., 2022. Mangrove microbiota along
584 the urban-to-rural gradient of the Cayenne estuary (French Guiana, South America): Drivers and potential
585 bioindicators. Sci. Total Environ. 807, 150667. https://doi.org/10.1016/j.scitotenv.2021.150667
586 Fierer, N., Bradford, M.A., Jackson, R.B., 2007. Toward an ecological classification of soil bacteria. Ecology 88,
587 1354–1364. https://doi.org/10.1890/05-1839
588 Fontana, A., Patrone, V., Puglisi, E., Morelli, L., Bassi, D., Garuti, M., Rossi, L., Cappa, F., 2016. Effects of
589 geographic area, feedstock, temperature, and operating time on microbial communities of six full-scale biogas plants.
590 Bioresour. Technol. 218, 980–990. https://doi.org/10.1016/j.biortech.2016.07.058
591 Franco, N.R., Giraldo, M.Á., López-Alvarez, D., Gallo-Franco, J.J., Dueñas, L.F., Puentes, V., Castillo, A., 2020.
592 Bacterial composition and diversity in deep-sea sediments from the Southern Colombian Caribbean Sea. Diversity
593 13, 10. https://doi.org/10.3390/d13010010
594 Ge, Y., Lou, Y., Xu, M., Wu, C., Meng, J., Shi, L., Xia, F., Xu, Y., 2021. Spatial distribution and influencing factors
595 on the variation of bacterial communities in an urban river sediment. Environ. Pollut. 272, 115984.
596 https://doi.org/10.1016/j.envpol.2020.115984

597 Goffredi, S.K., Orphan, V.J., 2010. Bacterial community shifts in taxa and diversity in response to localized organic
598 loading in the deep sea. Environ. Microbiol. 12, 344–363. https://doi.org/10.1111/j.1462-2920.2009.02072.x
599 Grabowski, R.C., Droppo, I.G., Wharton, G., 2011. Erodibility of cohesive sediment: The importance of sediment
600 properties. Earth-Sci. Rev. 105, 101–120. https://doi.org/10.1016/j.earscirev.2011.01.008
601 Gu, Z., 2022. Complex heatmap visualization. iMeta 1. https://doi.org/10.1002/imt2.43
602 Gu, Z., Eils, R., Schlesner, M., 2016. Complex heatmaps reveal patterns and correlations in multidimensional
603 genomic data. Bioinformatics 32, 2847–2849. https://doi.org/10.1093/bioinformatics/btw313
604 Gugliandolo, C., Michaud, L., Lo Giudice, A., Lentini, V., Rochera, C., Camacho, A., Maugeri, T.L., 2016.
605 Prokaryotic community in lacustrine sediments of byers peninsula (Livingston Island, Maritime Antarctica). Microb.
606 Ecol. 71, 387–400. https://doi.org/10.1007/s00248-015-0666-8
607 Guo, X., Niu, Z., Lu, D., Feng, J., Chen, Y., Tou, F., Liu, M., Yang, Y., 2017. Bacterial community structure in the
608 intertidal biofilm along the Yangtze Estuary, China. Mar. Pollut. Bull. 124, 314–320.
609 https://doi.org/10.1016/j.marpolbul.2017.07.051
610 Guo, X., Sun, X., Chen, Y., Hou, L., Liu, M., Yang, Y., 2020. Antibiotic resistance genes in biofilms on plastic wastes
611 in an estuarine environment. Sci. Total Environ. 745, 140916. https://doi.org/10.1016/j.scitotenv.2020.140916
612 Hillyer, K.E., Raes, E., Bissett, A., Beale, D.J., 2023. Multi-omics eco-surveillance of bacterial community function
613 in legacy contaminated estuary sediments. Environ. Pollut. 318, 120857.
614 https://doi.org/10.1016/j.envpol.2022.120857
615 Hou, Y., Li, B., Feng, G., Zhang, C., He, J., Li, H., Zhu, J., 2021. Responses of bacterial communities and organic
616 matter degradation in surface sediment to *Macrobrachium nipponense* bioturbation. Sci. Total Environ. 759, 143534.
617 https://doi.org/10.1016/j.scitotenv.2020.143534
618 Huergo, L.F., Rissi, D.V., Elias, A.S., Gonçalves, M.V., Gernet, M.V., Barreto, F., Dahmer, G.W., Reis, R.A., Pedrosa,
619 F.O., Souza, E.M., Monteiro, R.A., Baura, V.A., Balsanelli, E., Cruz, L.M., 2018. Influence of ancient anthropogenic
620 activities on the mangrove soil microbiome. Sci. Total Environ. 645, 1–9.
621 https://doi.org/10.1016/j.scitotenv.2018.07.094
622 Ismail, N., Almutairi, A., 2022. Bacterioplankton community profiling of the surface waters of Kuwait. Front. Mar.
623 Sci. 9, 838101. https://doi.org/10.3389/fmars.2022.838101
624 Kaestli, M., Skillington, A., Kennedy, K., Majid, M., Williams, D., McGuinness, K., Munksgaard, N., Gibb, K.,
625 2017. Spatial and temporal microbial patterns in a tropical macrotidal estuary subject to urbanization. Front.
626 Microbiol. 8, 1313. https://doi.org/10.3389/fmicb.2017.01313
627 Kallmeyer, J., Pockalny, R., Adhikari, R.R., Smith, D.C., D'Hondt, S., 2012. Global distribution of microbial
628 abundance and biomass in subseafloor sediment. Proc. Natl. Acad. Sci. 109, 16213–16216.
629 https://doi.org/10.1073/pnas.1203849109
630 Kessler, A.J., Chen, Y.-J., Waite, D.W., Hutchinson, T., Koh, S., Popa, M.E., Beardall, J., Hugenholtz, P., Cook,
631 P.L.M., Greening, C., 2019. Bacterial fermentation and respiration processes are uncoupled in anoxic permeable
632 sediments. Nat. Microbiol. 4, 1014–1023. https://doi.org/10.1038/s41564-019-0391-z
633 Kessler, A.J., Glud, R.N., Cardenas, M.B., Cook, P.L.M., 2013. Transport zonation limits coupled nitrification-
634 denitrification in permeable sediments. Environ. Sci. Technol. 47, 13404–13411. https://doi.org/10.1021/es403318x
635 Lai, X., Li, X., Song, J., Yuan, H., Duan, L., Li, N., Wang, Y., 2023. Nitrogen loss from the coastal shelf of the East
636 China Sea: Implications of the organic matter. Sci. Total Environ. 854, 158805.
637 https://doi.org/10.1016/j.scitotenv.2022.158805
638 Li, C., Adebayo, O., Ferguson, D.K., Wang, S., Rattray, J.E., Fowler, M., Webb, J., Campbell, C., Morrison, N.,
639 MacDonald, A., Hubert, C.R.J., 2023. Bacterial anomalies associated with deep sea hydrocarbon seepage along the
640 Scotian Slope. Deep Sea Res. Part Oceanogr. Res. Pap. 193, 103955. https://doi.org/10.1016/j.dsr.2022.103955

641 Li, M., Mi, T., Yu, Z., Ma, M., Zhen, Y., 2020. Planktonic bacterial and archaeal communities in an artificially
642 irrigated estuarine wetland: diversity, distribution, and responses to environmental parameters. Microorganisms 8,
643 198. https://doi.org/10.3390/microorganisms8020198
644 Li, M., Wei, G., Liu, J., Wang, X., Hou, L., Gao, Z., 2022. Effects of nitrate exposure on nitrate reduction processes
645 in the wetland sediments from the Yellow River estuary. Estuaries Coasts 45, 315–330.
646 https://doi.org/10.1007/s12237-021-00966-7
647 Liang, X., Peng, L.-H., Zhang, S., Zhou, S., Yoshida, A., Osatomi, K., Bellou, N., Guo, X.-P., Dobretsov, S., Yang,
648 J.-L., 2019. Polyurethane, epoxy resin and polydimethylsiloxane altered biofilm formation and mussel settlement.
649 Chemosphere 218, 599–608. https://doi.org/10.1016/j.chemosphere.2018.11.120
650 Liaw, A., Wiener, M., 2002. Classification and regression by randomForest. R News 2, 18–22.
651 Lindh, M.V., Sjöstedt, J., Andersson, A.F., Baltar, F., Hugerth, L.W., Lundin, D., Muthusamy, S., Legrand, C.,
652 Pinhassi, J., 2015. Disentangling seasonal bacterioplankton population dynamics by high-frequency sampling: High-
653 resolution temporal dynamics of marine bacteria. Environ. Microbiol. 17, 2459–2476. https://doi.org/10.1111/1462-
654 2920.12720
655 Liu, C., Zhao, D., Ma, W., Guo, Y., Wang, A., Wang, Q., Lee, D.-J., 2016. Denitrifying sulfide removal process on
656 high-salinity wastewaters in the presence of *Halomonas* sp. Appl. Microbiol. Biotechnol. 100, 1421–1426.
657 https://doi.org/10.1007/s00253-015-7039-6
658 Liu, W., Xie, W., Zhao, Q., Zhu, K., Yu, R., 2014. Spatial distribution and ecological stoichiometry characteristics
659 of carbon, nitrogen and phosphorus in soil in *Phragmites australis* tidal flat of Jiaozhou Bay. Wetl. Sci.
660 https://doi.org/10.13248/j.cnki.wetlandsci.2014.03.014
661 Liu, X., Wu, J., Hong, Y., Jiao, L., Li, Y., Wang, L., Wang, Y., Chang, X., 2020. Nitrogen loss by *nirS*-type
662 denitrifying bacterial communities in eutrophic coastal sediments. Int. Biodeterior. Biodegrad. 150, 104955.
663 https://doi.org/10.1016/j.ibiod.2020.104955
664 Liu, Y.-X., Qin, Y., Chen, T., Lu, M., Qian, X., Guo, X., Bai, Y., 2021. A practical guide to amplicon and metagenomic
665 analysis of microbiome data. Protein Cell 12, 315–330. https://doi.org/10.1007/s13238-020-00724-8
666 Louca, S., Parfrey, L.W., Doebeli, M., 2016. Decoupling function and taxonomy in the global ocean microbiome.
667 Science 353, 1272–1277. https://doi.org/10.1126/science.aaf4507
668 Lu, M., Wang, X., Li, H., Jiao, J.J., Luo, X., Luo, M., Yu, S., Xiao, K., Li, X., Qiu, W., Zheng, C., 2022. Microbial
669 community assembly and co-occurrence relationship in sediments of the river-dominated estuary and the adjacent
670 shelf in the wet season. Environ. Pollut. 308, 119572. https://doi.org/10.1016/j.envpol.2022.119572
671 Luo, G., Fotidis, I.A., Angelidaki, I., 2016. Comparative analysis of taxonomic, functional, and metabolic patterns
672 of microbiomes from 14 full-scale biogas reactors by metagenomic sequencing and radioisotopic analysis.
673 Biotechnol. Biofuels 9, 51. https://doi.org/10.1186/s13068-016-0465-6
674 Lv, X., Ma, B., Yu, J., Chang, S.X., Xu, J., Li, Y., Wang, G., Han, G., Bo, G., Chu, X., 2016. Bacterial community
675 structure and function shift along a successional series of tidal flats in the Yellow River Delta. Sci. Rep. 6, 36550.
676 https://doi.org/10.1038/srep36550
677 Lyu, F., Han, F., Ge, C., Mao, W., Chen, L., Hu, H., Chen, G., Lang, Q., Fang, C., 2023. OmicStudio: A composable
678 bioinformatics cloud platform with real-time feedback that can generate high-quality graphs for publication. iMeta
679 2. https://doi.org/10.1002/imt2.85
680 Lyu, X., Zhao, C., Xia, C., Qiao, F., 2010. Numerical study of water exchange in the Jiaozhou Bay and the tidal
681 residual currents near the bay mouth. Acta Oceanol. Sin. 32, 20–30.
682 Magoč, T., Salzberg, S.L., 2011. FLASH: fast length adjustment of short reads to improve genome assemblies.
683 Bioinformatics 27, 2957–2963. https://doi.org/10.1093/bioinformatics/btr507
684 Mori, F., Umezawa, Y., Kondo, R., Nishihara, G.N., Wada, M., 2021. Potential oxygen consumption and community

685 composition of sediment bacteria in a seasonally hypoxic enclosed bay. PeerJ 9, e11836.
686 https://doi.org/10.7717/peerj.11836
687 Morriën, E., Hannula, S.E., Snoek, L.B., Helmsing, N.R., Zweers, H., de Hollander, M., Soto, R.L., Bouffaud, M.-
688 L., Buée, M., Dimmers, W., Duyts, H., Geisen, S., Girlanda, M., Griffiths, R.I., Jørgensen, H.-B., Jensen, J., Plassart,
689 P., Redecker, D., Schmelz, R.M., Schmidt, O., Thomson, B.C., Tisserant, E., Uroz, S., Winding, A., Bailey, M.J.,
690 Bonkowski, M., Faber, J.H., Martin, F., Lemanceau, P., de Boer, W., van Veen, J.A., van der Putten, W.H., 2017. Soil
691 networks become more connected and take up more carbon as nature restoration progresses. Nat. Commun. 8, 14349.
692 https://doi.org/10.1038/ncomms14349
693 Mougi, A., Kondoh, M., 2012. Diversity of interaction types and ecological community stability. Science 337, 349–
694 351. https://doi.org/10.1126/science.1220529
695 Narihiro, T., Nobu, M.K., Kim, N.-K., Kamagata, Y., Liu, W.-T., 2015. The nexus of syntrophy-associated microbiota
696 in anaerobic digestion revealed by long-term enrichment and community survey: Microbial community of syntrophic
697 enrichment cultures. Environ. Microbiol. 17, 1707–1720. https://doi.org/10.1111/1462-2920.12616
698 Nocker, A., Lepo, J.E., Martin, L.L., Snyder, R.A., 2007. Response of estuarine biofilm microbial community
699 development to changes in dissolved oxygen and nutrient concentrations. Microb. Ecol. 54, 532–542.
700 https://doi.org/10.1007/s00248-007-9236-z
701 Offret, C., Gauthier, O., Despréaux, G., Bidault, A., Corporeau, C., Miner, P., Petton, B., Pernet, F., Fabioux, C.,
702 Paillard, C., Le Blay, G., 2023. Microbiota of the digestive glands and extrapallial fluids of clams evolve differently
703 over time depending on the intertidal position. Microb. Ecol. 85, 288–297. https://doi.org/10.1007/s00248-022-
704 01959-0
705 Oksanen, J., 2010. Vegan: community ecology package.
706 Oyetibo, G.O., Ige, O.O., Obinani, P.K., Amund, O.O., 2021. Ecological risk potentials of petroleum hydrocarbons
707 and heavy metals shape the bacterial communities of marine hydrosphere at Atlantic Ocean, Atlas Cove, Nigeria. J.
708 Environ. Manage. 289, 112563. https://doi.org/10.1016/j.jenvman.2021.112563
709 Parks, D.H., Tyson, G.W., Hugenholtz, P., Beiko, R.G., 2014. STAMP: statistical analysis of taxonomic and
710 functional profiles. Bioinformatics 30, 3123–3124. https://doi.org/10.1093/bioinformatics/btu494
711 Paterson, D.M., 1989. Short-term changes in the erodibility of intertidal cohesive sediments related to the migratory
712 behavior of epipelic diatoms. Limnol. Oceanogr. 34, 223–234. https://doi.org/10.4319/lo.1989.34.1.0223
713 Pearce, D., Hodgson, D., Thorne, M., Burns, G., Cockell, C., 2013. Preliminary analysis of life within a former
714 subglacial lake sediment in Antarctica. Diversity 5, 680–702. https://doi.org/10.3390/d5030680
715 Precht, E., Franke, U., Polerecky, L., Huettel, M., 2004. Oxygen dynamics in permeable sediments with wave-driven
716 pore water exchange. Limnol. Oceanogr. 49, 693–705. https://doi.org/10.4319/lo.2004.49.3.0693
717 Qian, P.-Y., Lau, S.C.K., Dahms, H.-U., Dobretsov, S., Harder, T., 2007. Marine biofilms as mediators of colonization
718 by marine macroorganisms: implications for antifouling and aquaculture. Mar. Biotechnol. 9, 399–410.
719 https://doi.org/10.1007/s10126-007-9001-9
720 Regnell, O., Watras, Carl.J., 2019. Microbial mercury methylation in aquatic environments: a critical review of
721 published field and laboratory studies. Environ. Sci. Technol. 53, 4–19. https://doi.org/10.1021/acs.est.8b02709
722 Reji, L., Tolar, B.B., Chavez, F.P., Francis, C.A., 2020. Depth-differentiation and seasonality of planktonic microbial
723 assemblages in the Monterey Bay upwelling system. Front. Microbiol. 11, 1075.
724 https://doi.org/10.3389/fmicb.2020.01075
725 Rickard, A.H., McBain, A.J., Stead, A.T., Gilbert, P., 2004. Shear rate moderates community diversity in freshwater
726 biofilms. Appl. Environ. Microbiol. 70, 7426–7435. https://doi.org/10.1128/AEM.70.12.7426-7435.2004
727 Roggatz, C.C., Parsons, D.R., 2022. Potential climate change impacts on the abiotic degradation of acyl-homoserine
728 lactones in the fluctuating conditions of marine biofilms. Front. Mar. Sci. 9, 882428.

https://doi.org/10.3389/fmars.2022.882428

Saad, S., Bhatnagar, S., Tegetmeyer, H.E., Geelhoed, J.S., Strous, M., Ruff, S.E., 2017. Transient exposure to oxygen or nitrate reveals ecophysiology of fermentative and sulfate-reducing benthic microbial populations: Ecophysiology of benthic microbial populations. Environ. Microbiol. 19, 4866–4881. https://doi.org/10.1111/1462-2920.13895

Shang, H., Xi, M., Li, Y., Kong, F., Wang, S., 2018. Evaluation of changes in the ecosystem services of Jiaozhou Bay coastal wetland. Acta Ecol. Sin. 38, 421–431. https://doi.org/10.5846/stxb201608301763

Suh, S.-S., Park, M., Hwang, J., Kil, E.-J., Jung, S.W., Lee, S., Lee, T.-K., 2015. Seasonal dynamics of marine microbial community in the South Sea of Korea. PLOS ONE 10, e0131633. https://doi.org/10.1371/journal.pone.0131633

Sun, J., Wei, L., Yin, R., Jiang, F., Shang, C., 2020. Microbial iron reduction enhances in-situ control of biogenic hydrogen sulfide by FeOOH granules in sediments of polluted urban waters. Water Res. 171, 115453. https://doi.org/10.1016/j.watres.2019.115453

Sun, Q., Song, J., Li, X., Yuan, H., Xing, J., 2021. Spatial variations of bacterial community composition in sediments of the Jiaozhou Bay, China. J. Oceanol. Limnol. 39, 865–879. https://doi.org/10.1007/s00343-020-0127-1

Tavares, T.C.L., Bezerra, W.M., Normando, L.R.O., Rosado, A.S., Melo, V.M.M., 2021. Brazilian semi-arid mangroves-associated microbiome as pools of richness and complexity in a changing world. Front. Microbiol. 12, 715991. https://doi.org/10.3389/fmicb.2021.715991

Taylor, H.B., Kurtz, H.D., 2020. Microbial community structure shows differing levels of temporal stability in intertidal beach sands of the grand strand region of South Carolina. PLOS ONE 15, e0229387. https://doi.org/10.1371/journal.pone.0229387

Tebbe, D.A., Geihser, S., Wemheuer, B., Daniel, R., Schäfer, H., Engelen, B., 2022. Seasonal and zonal succession of bacterial communities in North Sea salt marsh sediments. Microorganisms 10, 859. https://doi.org/10.3390/microorganisms10050859

Thomas, F.A., Sinha, R.K., Krishnan, K.P., 2020. Bacterial community structure of a glacio-marine system in the Arctic (Ny-Ålesund, Svalbard). Sci. Total Environ. 718, 135264. https://doi.org/10.1016/j.scitotenv.2019.135264

Thomson, T., Ellis, J.I., Fusi, M., Prinz, N., Bennett-Smith, M.F., Aylagas, E., Carvalho, S., Jones, B.H., 2022. The right place at the right time: Seasonal variation of bacterial communities in arid Avicennia marina soils in the Red Sea is specific to its position in the intertidal. Front. Ecol. Evol. 10, 845611. https://doi.org/10.3389/fevo.2022.845611

van de Kamp, J., Hook, S.E., Williams, A., Tanner, J.E., Bodrossy, L., 2019. Baseline characterization of aerobic hydrocarbon degrading microbial communities in deep-sea sediments of the Great Australian Bight, Australia. Environ. Microbiol. 21, 1782–1797. https://doi.org/10.1111/1462-2920.14559

Wahl, M., Goecke, F., Labes, A., Dobretsov, S., Weinberger, F., 2012. The second skin: ecological role of epibiotic biofilms on marine organisms. Front. Microbiol. 3. https://doi.org/10.3389/fmicb.2012.00292

Wang, H., Zhang, C., Chen, F., Kan, J., 2020. Spatial and temporal variations of bacterioplankton in the Chesapeake Bay: A re-examination with high-throughput sequencing analysis. Limnol. Oceanogr. 65, 3032–3045. https://doi.org/10.1002/lno.11572

Wang, Y., Zhang, C., Qi, L., Jia, X., Lu, W., 2016. Diversity and antimicrobial activities of cultivable bacteria isolated from Jiaozhou Bay. Acta Microbiol. Sin. https://doi.org/10.13343/j.cnki.wsxb.20160132

Wang, Z., Gao, S., Sun, Z., Zhang, Y., Zhang, X., 2022. Study on the effects of rainfall and ecological water supplement on the pollutant transport in Licun River. Trans. Oceanol. Limnol. https://doi.org/10.13984/j.cnki.cn37-1141.2022.03.012

Wei, W., Isobe, K., Nishizawa, T., Zhu, L., Shiratori, Y., Ohte, N., Koba, K., Otsuka, S., Senoo, K., 2015. Higher diversity and abundance of denitrifying microorganisms in environments than considered previously. ISME J. 9,

1954–1965. https://doi.org/10.1038/ismej.2015.9

Wei, Z., Liu, Y., Feng, K., Li, S., Wang, S., Jin, D., Zhang, Y., Chen, H., Yin, H., Xu, M., Deng, Y., 2018. The divergence between fungal and bacterial communities in seasonal and spatial variations of wastewater treatment plants. Sci. Total Environ. 628–629, 969–978. https://doi.org/10.1016/j.scitotenv.2018.02.003

Whitehouse, R., 2000. Dynamics of estuarine muds: A manual for practical applications. Thomas Telford.

Wu, D., Huang, X.-H., Sun, J.-Z., Graham, D.W., Xie, B., 2017. Antibiotic resistance genes and associated microbial community conditions in aging landfill systems. Environ. Sci. Technol. 51, 12859–12867. https://doi.org/10.1021/acs.est.7b03797

Wu, J., Hong, Y., Ye, J., Li, Yiben, Liu, X., Jiao, L., Li, T., Li, Yuwei, Bin, L., Wang, Y., 2019. Diversity of anammox bacteria and contribution to the nitrogen loss in surface sediment. Int. Biodeterior. Biodegrad. 142, 227–234. https://doi.org/10.1016/j.ibiod.2019.05.018

Wyness, A.J., Paterson, D.M., Rimmer, J.E.V., Defew, E.C., Stutter, M.I., Avery, L.M., 2019. Assessing risk of *E. coli* resuspension from intertidal estuarine sediments: implications for water quality. Int. J. Environ. Res. Public. Health 16, 3255. https://doi.org/10.3390/ijerph16183255

Yi, J., Lo, L.S.H., Cheng, J., 2020. Dynamics of microbial community structure and ecological functions in estuarine intertidal sediments. Front. Mar. Sci. 7, 585970. https://doi.org/10.3389/fmars.2020.585970

Zhang, J., Zhang, N., Liu, Y.-X., Zhang, X., Hu, B., Qin, Y., Xu, H., Wang, H., Guo, X., Qian, J., Wang, W., Zhang, P., Jin, T., Chu, C., Bai, Y., 2018. Root microbiota shift in rice correlates with resident time in the field and developmental stage. Sci. China Life Sci. 61, 613–621. https://doi.org/10.1007/s11427-018-9284-4

Zhang, W., Tang, J., Liang, B., 2017. Numerical study on the influence of the forebay reclamation on pollutant transport in the Jiaozhou bay. Mar. Environ. Sci. https://doi.org/10.13634/j.cnki.mes.2017.01.005

Zhang, X., Hu, B.X., Ren, H., Zhang, J., 2018. Composition and functional diversity of microbial community across a mangrove-inhabited mudflat as revealed by 16S rDNA gene sequences. Sci. Total Environ. 633, 518–528. https://doi.org/10.1016/j.scitotenv.2018.03.158

Zhou, Z., Meng, H., Liu, Y., Gu, J.-D., Li, M., 2017. Stratified bacterial and archaeal community in mangrove and intertidal wetland mudflats revealed by high throughput 16S rRNA gene sequencing. Front. Microbiol. 8, 2148. https://doi.org/10.3389/fmicb.2017.02148

Zhuang, L., Tang, Z., Ma, J., Yu, Z., Wang, Y., Tang, J., 2019. Enhanced anaerobic biodegradation of benzoate under sulfate-reducing conditions with conductive iron-oxides in sediment of Pearl River Estuary. Front. Microbiol. 10, 374. https://doi.org/10.3389/fmicb.2019.00374

Zinke, L.A., Mullis, M.M., Bird, J.T., Marshall, I.P.G., Jørgensen, B.B., Lloyd, K.G., Amend, J.P., Kiel Reese, B., 2017. Thriving or surviving? Evaluating active microbial guilds in Baltic Sea sediment: Baltic Sea sediment metatranscriptomes. Environ. Microbiol. Rep. 9, 528–536. https://doi.org/10.1111/1758-2229.12578